Nanoscale

PAPER

View Article Online
View Journal | View Issue

Wearable multifunctional sensors using printed stretchable conductors made of silver nanowires†

Cite this: *Nanoscale*, 2014, **6**, 2345

Shanshan Yao and Yong Zhu*

Considerable efforts have been made to achieve highly sensitive and wearable sensors that can simultaneously detect multiple stimuli such as stretch, pressure, temperature or touch. Here we develop highly stretchable multifunctional sensors that can detect strain (up to 50%), pressure (up to ~1.2 MPa) and finger touch with high sensitivity, fast response time (~40 ms) and good pressure mapping function. The reported sensors utilize the capacitive sensing mechanism, where silver nanowires are used as electrodes (conductors) and Ecoflex is used as a dielectric. The silver nanowire electrodes are screen printed. Our sensors have been demonstrated for several wearable applications including monitoring thumb movement, sensing the strain of the knee joint in patellar reflex (knee-jerk) and other human motions such as walking, running and jumping from squatting, illustrating the potential utilities of such sensors in robotic systems, prosthetics, healthcare and flexible touch panels.

Received 16th October 2013
Accepted 2nd December 2013

DOI: 10.1039/c3nr05496a

www.rsc.org/nanoscale

1. Introduction

With the recent progress of robotic systems, prosthetics and wearable medical devices, efforts have been devoted towards realization of highly sensitive and skin-mountable sensors.[1–3] Among the various sensing capabilities, strain, pressure and touch sensation are of great importance in several steps involved in human–robot interaction loops.[1] They could help the robotics and prosthetic devices understand how real-world objects "feel" during interactions, obtain biosignals such as finger touching and body motions sent from humans to control robotics and prosthetic devices, and provide feedback information during actuating.[1,4,5] Besides the utilities in robotic systems and prosthetics, wearable sensors that can be embedded into clothes or directly wrapped around non-planar and biological surfaces[6] are widely used to monitor human body motions and offer new opportunities for real-time health/wellness monitoring.[3,7,8] For those applications mentioned above, stretchability of the sensors is generally required in addition to flexibility.[1,3,9]

Much progress has been made to develop wearable sensors for robotics, prosthetics and medical applications. Arrays of flexible artificial skins based on pressure sensitive rubber (PSR) were fabricated, either with organic field-effect transistors (OFETs)[10] or with ordered inorganic semiconductor nanowire transistors,[11] capable of monitoring pressure with a spatial resolution of ~2.5 mm. Similar OFETs-based electronic skins with a net-shaped structure, which could detect pressure and temperature simultaneously and could be stretched by 25% were reported.[12] However, those PSR-based pressure sensors are commonly susceptible to hysteresis.[1,13] Pressure and strain sensing were simultaneously achieved recently in multilayered microchannels filled with conductive liquid[14] and in capacitive sensors using carbon nanotubes as electrodes.[6] The pressure response of the former one was nonlinear while the sensitivity of the latter one was relatively low. To achieve better understanding of the environment and more effective feedback control, the robotics and prosthetics will greatly benefit from stretchable sensors with multiple functions. Pang *et al.* achieved detection of pressure, shear and torsion using interlocked arrays of nanofibres and demonstrated potentials for wearable health monitoring.[15] Cotton *et al.* developed stretchable capacitive sensors, enabling detection of strain up to 20%, a pressure up to 160 kPa and human touch.[2] Yet effective, the strechability of the sensors could be further improved by replacing the gold films with more stretchable conductors. So far, very few multifunctional wearable sensors based on silver nanowires have been developed.[16]

In this paper, we present multifunctional wearable sensors based on highly conductive and stretchable silver nanowire (AgNW) conductors, which enable the detection of the strain (up to 50%), pressure (up to ~1.2 MPa) and finger touch on a simple platform. The sensors exibit large stretchability, high sensitivity, fast response time (~40 ms) and good pressure mapping function. Such sensors can be readily mounted onto human bodies to monitor the skin strain associated with thumb flexing, knee jerk and other human motions including walking, running and jumping from squatting. Moreover, the fabrication process is simple and easy to be extended for fabricating complex, large area sensors.

Department of Mechanical and Aerospace Engineering, North Carolina State University, Raleigh, NC 27695, USA. E-mail: yong_zhu@ncsu.edu

† Electronic supplementary information (ESI) available. See DOI: 10.1039/c3nr05496a

2. Results and discussion

The fabrication process of an array of capacitive sensors is schematically illustrated in Fig. 1a. The parallel AgNW conductors have a linewidth of ~2 mm and a spacing of ~2 mm. The AgNW, polydimethylsiloxane (PDMS) and the dielectric layer as shown in Fig. 1b are about 5 μm, 0.2 mm and 0.5 mm in thickness, respectively. An individual capacitive sensor can be fabricated following the same process. The principles for strain sensing, pressure sensing and touch sensing to be discussed later are schematically shown in Fig. 2.

2.1. Strain sensing

Each capacitive sensor can be treated as a parallel-plate capacitor with the overlapped length l_0, width w_0, and separation d_0 between the electrodes (*i.e.*, thickness of the dielectric layer). The initial capacitance is given by

$$C_0 = \varepsilon_0 \varepsilon_r \frac{l_0 w_0}{d_0} \quad (1)$$

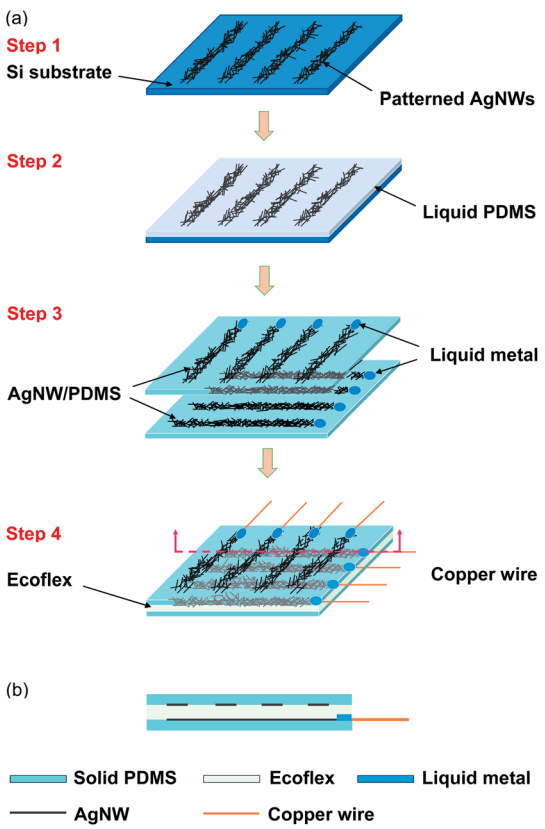

Fig. 1 (a) Fabrication process flow of the capacitive multifunctional sensors. Step 1: print AgNW stretchable conductors patterned by screen printing. Step 2: drop cast liquid PDMS and cure the structure. Peel off the AgNW/PDMS film from the Si substrate. Step 3: drop liquid metal (EGaIn) to make conformal contact with the terminals of the AgNW conductors. Step 4: position two pieces of AgNW/PDMS films orthogonally with AgNWs face to face. Laminate two AgNW/PDMS films together with Ecoflex, embed copper wires and cover liquid metal with liquid Ecoflex. The whole piece is cured at room temperature. (b) Cross-sectional view of the sensor. The schematics are not drawn to scale.

where ε_0 and ε_r are the electric constant and dielectric constant for the dielectric layer, respectively. As the sensor is uniaxially stretched to strain ε, the length (along the strain direction) of the electrode increases to $(1 + \varepsilon)l_0$, while the width of the electrode and the separation between the two electrodes decrease to $(1 - \nu_{PDMS}\varepsilon)w_0$ and $(1 - \nu_{Ecoflex}\varepsilon)d_0$, where ν_{PDMS} and $\nu_{Ecoflex}$ are the Poisson ratios of the PDMS and Ecoflex, respectively. Assuming ν_{PDMS} and $\nu_{Ecoflex}$ are both 0.5, the capacitance as a result of the tensile strain is now estimated to be

$$C = \varepsilon_0 \varepsilon_r \frac{(1+\varepsilon) l_0 (1 - \nu_{PDMS}\varepsilon) w_0}{(1 - \nu_{Ecoflex}\varepsilon) d_0} \approx \varepsilon_0 \varepsilon_r \frac{(1+\varepsilon) l_0 w_0}{d_0} = (1+\varepsilon) C_0 \quad (2)$$

The capacitance was measured by an AD7152 capacitance-to-digital converters (CDCs) evaluation board (Analog Devices), which has the offset calibration function to compensate parasitic capacitance from the lead wires and the surrounding environment. Fig. 3a shows the relative capacitance change $\Delta C/C_0$ *versus* tensile strain during stretching and releasing. The strain sensor exhibited good linearity and reversibility up to a very large strain level (*e.g.*, 50% as demonstrated here). In addition, the sensor exhibited excellent stability after many stretching/releasing cycles, as shown in Fig. 3b.

Similar to resistive strain gauges, here we define the capacitive gauge factor as the relative change in capacitance divided by the mechanical strain. The theoretical value is given by

$$GF = \frac{\Delta C}{C_0 \varepsilon} \approx \frac{(1+\varepsilon) C_0 - C_0}{C_0 \varepsilon} = 1 \quad (3)$$

However, the gauge factor of our strain sensors was found to be ~0.7. Gauge factors reported for most of the capacitive strain sensors are less than the theoretical value of 1. For instance, the sensor with sprayed CNT films as electrodes and Ecoflex as dielectrics had a gauge factor of 0.4 (ref. 6) and that made of gold thin films separated by PDMS had 0.75.[2] Strain sensors based on the resistive mechanism usually suffer from large hysteresis and nonlinearity under large strain.[15,17] For our capacitive sensors, the hysteresis was found to be negligible. In addition, the sensors can reliably detect the strain below 1%. Of note is that parallel electrode configuration is commonly used in capacitive strain sensors.[2,18,19] Following the same fabrication process, we also fabricated strain sensors with the parallel configuration. As shown in Fig. S1,† the strain sensor with parallel AgNW electrodes also exhibited excellent linearity and a similar gauge factor.

The strain range during human movements is typically much larger than that of conventional strain gauges.[3,20,21] As reported by Wessendorf *et al.*,[21] the maximum skin strain associated with the knee joint for an entire flexion and the extension cycle (squatting and rising) was up to 44.6% in any direction. We demonstrated our sensors for large-strain measurements in various applications, as shown in Fig. 3c–g. Due to the flexibility and stretchability of our sensors, they can be easily mounted onto a curvilinear surface (*e.g.*, human body) with the aid of medical tape.

Fig. 3c shows the strain sensor placed onto a thumb for strain measurements. As indicated in Fig. 3d, the thumb of the

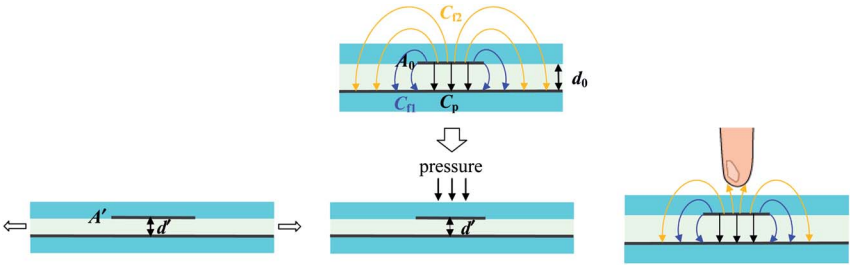

Fig. 2 Schematics showing the three sensing modalities: (top) the initial state, (bottom left) under strain, (bottom middle) under pressure and (bottom right) under finger touch. A_0, d_0 and A', d' represent the overlapped area of the electrodes and the separation between electrodes for the initial state and under the stimuli, respectively. The sensor capacitance has three contributions, C_p, C_{f1} and C_{f2} that represent the capacitance of parallel plates, the fringing capacitance in the Ecoflex and PDMS overlay, and the fringing capacitance through the medium above the sensor, respectively.[2]

person under test has a slight curvature on the thumb joint, when holding the thumb up naturally. The skin of the phalange was under a slight tension strain, leading to a slight increase in capacitance. When the thumb was straightened, it actually relaxed and the strain decreased, accompanied by a decrease in capacitance. Then the person changed the gesture to a fist, and the thumb joints experienced increased strain. As a result, the sensor showed large increase in capacitance (*e.g.*, 25% that corresponds to 36% tensile strain). From the capacitance measurement, here we clearly obtain the skin strain involved in thumb flexure. Multiple sensors can be mounted onto other finger joints similarly. The measured strain signals could be used as a feedback for robotics or prosthetic devices to realize better human control.[1]

Patellar reflex or knee-jerk is very useful in early diagnoses of nervous system diseases. The absence of patellar reflex, known as Westphal's sign, could be a symptom of diseases such as tabes dorsalis and receptor damage.[22] On the other hand, a pendular knee-jerk could be associated with hypotonia.[23] As the second demonstration, patellar reflex was monitored using our wearable sensors. A sensor was attached onto the knee while the person was sitting with the lower leg relaxed naturally. Initially the sensor experienced a large tensile strain across the knee. To test the patellar reflex, a hammer was used to tap the patellar tendon ligament. As a response, the lower leg should straighten involuntarily in a sudden kicking motion, as illustrated in Fig. 3e, and then come to rest quickly. It can be seen that upon tapping, a sudden decrease in capacitance was observed, corresponding to the release of the capacitive sensor (from the tension state) as a result of the quick kicking movement. With the relaxation of the knee, the capacitance returned to the initial value. Fig. 3f represents the capacitance change for a normal knee jerk, without the sign of absent or pendular knee-jerk. The amplitude and duration of the kicking motion in response to a given tapping could provide valuable information for early diagnoses of nervous system diseases.

By mounting the sensors on the knee, the reported strain sensors can also be used to detect other human motions, such as walking, running and jumping from squatting, as shown in Fig. 3g. Above discussed applications demonstrated that through real-time strain measurements, our skin-mountable sensors can help in monitoring the body motions, which provides important information for feedback control in robotic systems and prosthetic devices.[1] At the same time, the sensors could be beneficial for continuous health/wellness monitoring, for example, to help in detecting physiological conditions (such as knee-jerk) for diagnoses, to monitor body motions during rehabilitation, and to quantize the body movement to evaluate an athlete's performance.[38]

2.2. Pressure sensing

A 7 × 7 array of capacitors ('pixels') was fabricated following the process shown in Fig. 1 to form a pressure sensor that has spatial resolution. When a pressure is applied on the capacitor, the separation between the two AgNW layers decreases, resulting in an increase in capacitance (as shown in Fig. 2). The relative change in capacitance of one pixel as a function of the pressure is presented in Fig. 4a. The relative capacitance change $\Delta C/C_0$ shows a bilinear dependence on the pressure. Pressure sensitivity S, defined as the slope of the traces,[24] is commonly used to evaluate the performance of a pressure sensor. For pressures below and above 500 kPa, the sensitivity of our sensors is 1.62 MPa^{-1} and 0.57 MPa^{-1}, respectively. Compared with previously reported capacitive pressure sensors, the sensitivity of our sensors is higher than those with carbon nanotube electrodes (0.23 MPa^{-1} over the pressure range up to ~1 MPa)[6] and those with serpentine gold electrodes (0.48 MPa^{-1} over the pressure range up to 0.25 MPa),[25] both using Ecoflex as dielectric layers. Our sensors are also more sensitive than those based on gold thin films embedded in silicone rubber (0.4 MPa^{-1} for pressure up to 160 kPa).[2] Several other capacitive sensors were demonstrated with higher sensitivity but had either poorer linearity or poorer stretchability. For example, pressure sensors composed of copper electrodes and air gaps encapsulated by PDMS showed a nonlinear response with a sensitivity of 3% mN^{-1} (4.8 MPa^{-1}) over the range of 40 mN (250 kPa).[26] The sensors with copper-clad laminated composites on an unstretchable polyimide substrate exhibited a sensitivity of 9.2 MPa^{-1} for the range of 40 kPa.[27] Highly sensitive pressure sensors using a microstructured PDMS dielectric layer and a PET substrate were reported by Mannsfeld *et al.*[24] The sensor showed a similar bilinear response (0.55 kPa^{-1} for less than 2 kPa and 0.15 kPa^{-1} for 2–7 kPa), but on the non-stretchable polyester substrate.

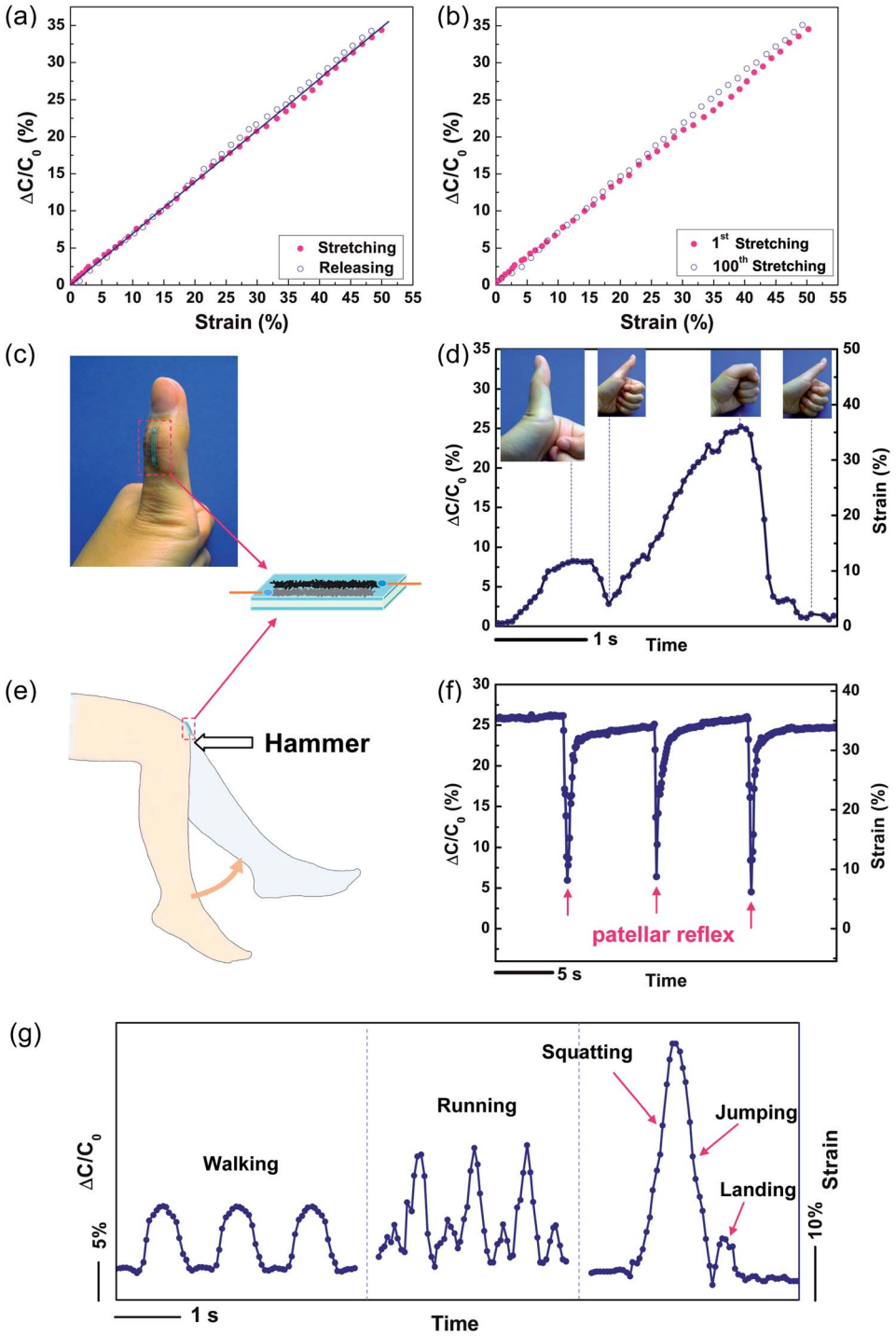

Fig. 3 Strain sensing capability of the fabricated capacitive sensors. (a) Relative capacitance change $\Delta C/C_0$ *versus* tensile strain for stretching and releasing. The solid line shows the linear fits to the data. (b) Relative capacitance change $\Delta C/C_0$ *versus* tensile strain for two measurements. The second measurement was done after the sensor was stretched and released for 100 cycles. (c–g) Demonstrations showing the large-strain sensing capability. (c) One pixel sensor on a thumb joint. (d) Relative capacitance change and strain associated with thumb flexure from holding thumb up to make a fist and back to a relaxed state. (e) Schematic of the patellar reflex experiment. (f) Relative capacitance change and strain caused by knee motion in patellar reflex. (g) Relative capacitance change and strain *versus* time for various human motions: walking, running and jumping from squatting.

Fast response time is important in realizing real-time pressure monitoring. We applied small loadings by dispersing three 0.06 g water droplets. The time response is shown in Fig. 4b. Here, the response time (rise time) is defined as the time interval between 10% and 90% of the steady state values.[28] Our response time was estimated to be around 40 ms (see ESI† for

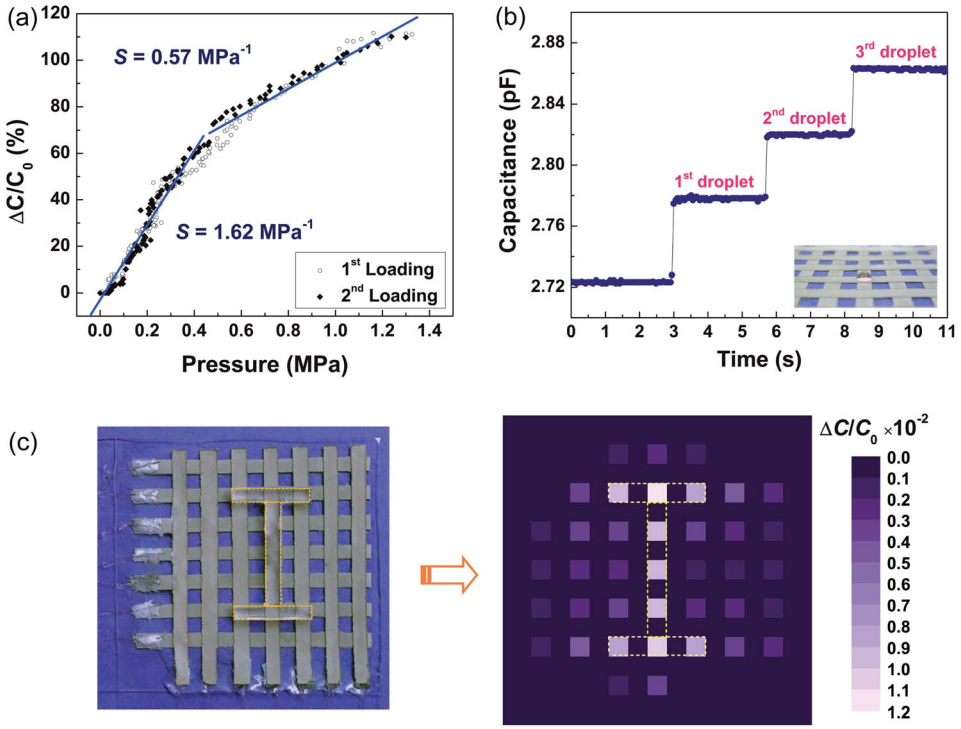

Fig. 4 Pressure sensing capability of the fabricated capacitive array. (a) Relative capacitance change $\Delta C/C_0$ of one pixel *versus* normal pressure for two consecutive measurements. (b) Response of the pressure sensor to water droplets with weight of 0.06 g each. Inset shows a water droplet on top of a sensor array in the middle. (c) The sensor array with a PDMS mold in the shape of "I" on top (left) and the resulting map of capacitance change (right).

calculation of the response time). Our response time is much shorter than those reported for other pressure sensors such as the flexible polymer foam based capacitive sensor (several seconds)[29] and the one using an Au film patterned on a PDMS membrane (~200 ms).[28]

Very few pressure sensors can simultaneously achieve the large stretchability, fast response, high sensitivity and good linearity. To demonstrate the function of measuring the spatial distribution of pressure, a 2.7 g mold with the shape of letter "I" was cut and placed onto the sensor. The resulting relative capacitance changes are plotted in Fig. 4c, where a brighter color corresponds to a higher capacitance change. Though the cross-talk (*i.e.*, the influence of the pixel on which pressure is applied on the adjacent pixels[6]) between different pixels exists, we can clearly identify the spatial distribution of the applied pressure.

2.3. Touch sensing

Besides strain and pressure sensing capabilities, our capacitive sensors can also be used to detect finger touch, to be more general, the touch of a grounded conducting medium.[2] Unlike the strain and pressure sensing, the capacitance change in touch sensing is due to the disturbance of the fringing electric field[2] rather than the dimension changes, as shown in Fig. 2. A similar mechanism is widely used in the capacitive touch screens.[30]

When a finger or other properly grounded conductors touch a capacitor, the fringing electric field (through the medium directly above the sensor) is partially intercepted and shunted to ground by the finger,[2,31] resulting in a decrease in capacitance. The sensor can function well as long as the finger is in the proximity of the electrode, no matter whether there is force applied onto the sensor or not. Here we differentiate the two situations as (1) proximity mode (no force applied) and (2) pressing mode (force is applied). Fig. 5a shows the response of one pixel in the sensor array to finger touch (no force applied). As expected the capacitance decreases upon finger touching. In order to probe the determining factors of the capacitance change, we approached the sensor from 30 cm away until touching the sensor with different finger areas to investigate the effects of the interacting areas and the distance between the finger and the pixel. Fig. 5c and d reveal that the capacitance change increases with increasing interaction area and decreasing distance. Larger interaction area and shorter distance lead to a larger capacitance decrease because of the increased portion of the electric field intercepted by the finger.

In some touch sensing applications, forces from finger touch are inevitable and it is more convenient if the sensor can be touched with whatever force the users like. Fig. 5b presents the results for two different modes, where the capacitance changes resulting from strong finger press (large force applied) and gentle finger touch (no force applied) were shown for comparison. In the pressing mode, the finger pressing has two opposing effects on the capacitance: finger as a grounded conductor leads to a decrease in the capacitance while physical pressing causes an increase in the capacitance as the pressure sensor does. The

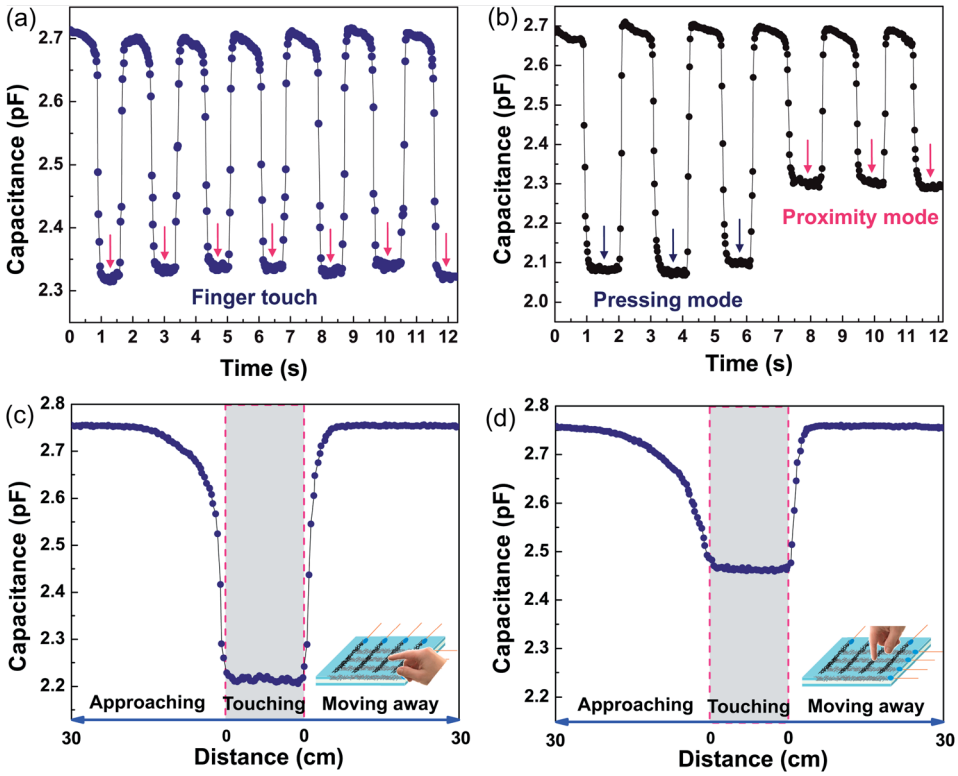

Fig. 5 Touch sensing capability of the fabricated capacitive sensors. (a) Change in capacitance for one pixel before and after repeated finger touching. (b) Change in capacitance for strong finger press (pressing mode) and gentle finger touch (proximity mode). (c) Capacitance change as a function of the distance between sensor and finger when the finger pad approaches and leaves the sensor. (d) Capacitance change as a function of the distance between sensor and finger when the fingertip approaches and leaves the sensor.

capacitance decrease caused by the disturbed electric field was found to be much larger than that by the physical pressing. This finding indicates that the sensor can be reliably used as a touch sensor under either proximity mode or pressing mode (*i.e.*, gentle or strong touches). For strong press, the interacting area between the finger and the pixel electrode is typically larger compared to gentle touch, which leads to a much larger capacitance decrease, as shown in Fig. 5c and d. The relative capacitance change of our touch sensor is comparable to those of capacitive touch sensors reported in the literature.[2] Flexible resistive[32] and piezoelectric[33] touch sensors were also reported, but the strechability were limited either by the sensing layer[33] or by the substrate material.[32] Moreover, those sensors can only be used when the finger presses the sensors. In contrast, the capacitive touch sensors have a longer detecting range; they can function as long as the finger is in proximity. This characteristic could be very useful in applications where contacts between robots and humans should be avoided. For example, they may be used to assist robots to navigate and avoid injuring humans.[31]

We have demonstrated the strain, pressure and touching sensing modalities using our capacitive sensors. The electrode, dielectric and substrate materials enable mechanical robust sensors that are stretchable and conformal to curvilinear surfaces. It is worth noting that as an advantage of using stretchable materials for pressure sensors, the existence of tensile strain and normal pressure could be distinguished from the distribution of capacitance changes.[6] Tensile straining affects all the pixels along the strain direction; in contrast, pressure only affects the pixels in the immediate vicinity of the load.[6] The existence of the finger touch can also be identified and distinguished because only finger touch causes the decrease in capacitance. According to the specific needs, all the pixels could have the three functions or different pixels may be engineered to have different localized functions.[2] In short, the multifunctional sensor offers more possibilities to meet the needs in diverse applications.

3. Conclusions

In summary, multifunctional wearable sensors based on stretchable AgNW conductors were developed following a simple and scalable fabrication process. The sensor showed a linear response to large tensile strain up to 50% with a gauge factor of ~0.7 and a bilinear response to pressure. The wearability of the sensor was demonstrated by mounting it onto human bodies to monitor the skin strain associated with finger flexing and knee motions in the patellar reflex and other body movements. In addition, the sensor exhibited fast response time (~40 ms) and good pressure mapping function. Moreover, the ability of sensing the finger touching was demonstrated. Performances of our proof-of-concept devices, such as the stability, sensitivity, linearity, detecting range or response time, could be further enhanced *via* optimization of geometry and materials. But this study opens up a route in terms of materials

and structures to develop stretchable sensors with multi-functionalities. The multifunctional sensors have potentials to be integrated with other wearable devices (*e.g.*, sensors,[34,35] actuators,[36,37] antennas,[38,39] and power devices[40,41]) and used as the conformal intelligent surfaces to interact with humans and the environments in robotic systems, prosthetics, wearable health monitoring devices or flexible touch pads.

4. Experimental section

4.1. Device fabrication

To fabricate the device, parallel AgNW conductors with a linewidth of ~2 mm and a spacing of ~2 mm were screen printed on top of a Si substrate through a pre-patterned PDMS shadow mask (Step 1 in Fig. 1). More details on the fabrication processes of the AgNW conductors were reported previously.[18] Liquid PDMS (mixing the "base" and the "curing agent" with a weight ratio of 10 : 1) was then cast onto the Si substrate that included the AgNW conductors on top, and cured at 65 °C for 12 hours. All the patterned AgNW conductors were embedded just below the PDMS surface when it was peeled off the Si substrate (Step 2). Eutectic gallium–indium (EGaIn, Aldrich, ≥99.99%) liquid metal was applied to the two ends of the AgNW/PDMS strips to serve as conformal electrodes. After that, the AgNW/PDMS film was positioned orthogonal to another identical AgNW/PDMS film face to face (Step 3). The Ecoflex silicone elastomer (Smooth-On, Inc., Shore hardness 00–10) was introduced as the dielectric layer of the capacitors, which is a very soft material that can help in increasing the sensitivity of the pressure sensor. Liquid Ecoflex made by mixing part A and part B with the ratio of 1 : 1 was applied between the two orthogonally positioned AgNW/PDMS films. At the same time, copper wires were embedded inside the liquid metal and covered by Ecoflex liquid. Finally, the whole structure was degassed in a vacuum oven followed by curing under ambient conditions for approximately 4 hours (Step 4). This way, the Ecoflex layer was sandwiched between the orthogonally patterned stretchable AgNW conductors to form the capacitive sensors.

Acknowledgements

This work was supported by the National Science Foundation through ASSIST Engineering Research Center (EEC-1160483). YZ acknowledges support from the US Department of Energy Nuclear Energy University Program (NEUP). The authors would like to thank Dr Feng Xu for his valuable suggestions in fabricating the pressure sensors.

References

1 N. Lu and D.-H. Kim, *Soft Robotics*, 2013, **1**, 53–62.
2 D. P. J. Cotton, I. M. Graz and S. P. Lacour, *IEEE Sens. J.*, 2009, **9**, 2008–2009.
3 T. Yamada, Y. Hayamizu, Y. Yamamoto, Y. Yomogida, A. Izadi-Najafabadi, D. N. Futaba and K. Hata, *Nat. Nanotechnol.*, 2011, **6**, 296–301.
4 R. S. Dahiya, G. Metta, M. Valle and G. Sandini, *IEEE Trans. Robot.*, 2010, **26**, 1–20.
5 M. I. Tiwana, S. J. Redmond and N. H. Lovell, *Sens. Actuators, A*, 2012, **179**, 17–31.
6 D. J. Lipomi, M. Vosgueritchian, B. C.-K. Tee, S. L. Hellstrom, J. A. Lee, C. H. Fox and Z. Bao, *Nat. Nanotechnol.*, 2011, **6**, 788–792.
7 N. Lu, C. Lu, S. Yang and J. Rogers, *Adv. Funct. Mater.*, 2012, **22**, 4044–4050.
8 U. Tata, H. Cao, V. Landge, C. M. Nguyen and J.-C. Chiao, *2013 IEEE Topical Conference on Bio-medical Wireless Technologies, Networks, and Sensing Systems*, Austin, 2013, pp. 23–25.
9 D.-H. Kim, R. Ghaffari, N. Lu and J. A. Rogers, *Annu. Rev. Biomed. Eng.*, 2012, **14**, 113–128.
10 T. Someya, T. Sekitani, S. Iba, Y. Kato, H. Kawaguchi and T. Sakurai, *Proc. Natl. Acad. Sci. U. S. A.*, 2004, **101**, 9966–9970.
11 K. Takei, T. Takahashi, J. C. Ho, H. Ko, A. G. Gillies, P. W. Leu, R. S. Fearing and A. Javey, *Nat. Mater.*, 2010, **9**, 821–826.
12 T. Someya, Y. Kato, T. Sekitani, S. Iba, Y. Noguchi, Y. Murase, H. Kawaguchi and T. Sakurai, *Proc. Natl. Acad. Sci. U. S. A.*, 2005, **102**, 12321–12325.
13 M. Hussain, Y.-H. Choa and K. Niihara, *J. Mater. Sci. Lett.*, 2001, **20**, 525–527.
14 Y.-L. Park, B. Chen and R. J. Wood, in *2011 IEEE Sensors Proceedings*, IEEE, 2011, vol. 2, pp. 81–84.
15 C. Pang, G.-Y. Lee, T. Kim, S. M. Kim, H. N. Kim, S.-H. Ahn and K.-Y. Suh, *Nat. Mater.*, 2012, **11**, 795–801.
16 W. Hu, X. Niu, R. Zhao and Q. Pei, *Appl. Phys. Lett.*, 2013, **102**, 083303.
17 K. Kim, K. R. Lee, W. H. Kim, K.-B. Park, T.-H. Kim, J.-S. Kim and J. J. Pak, *Sens. Actuators, A*, 2009, **156**, 284–291.
18 F. Xu and Y. Zhu, *Adv. Mater.*, 2012, **24**, 5117–5122.
19 D. J. Cohen, D. Mitra, K. Peterson and M. M. Maharbiz, *Nano Lett.*, 2012, **12**, 1821–1825.
20 K. Arshak, D. Morris, A. Arshak and O. Korostynska, *J. Mater. Sci.: Mater. Electron.*, 2006, **17**, 767–778.
21 A. M. Wessendorf and D. J. Newman, *IEEE Trans. Biomed. Eng.*, 2012, **59**, 3432–3438.
22 D. Jensen and B. Jensen, in *The principles of physiology*, Appleton-Century-Crofts, New York, 1976.
23 G. Holmes, *Brain*, 1939, **62**, 1–30.
24 S. C. B. Mannsfeld, B. C.-K. Tee, R. M. Stoltenberg, C. V. H.-H. Chen, S. Barman, B. V. O. Muir, A. N. Sokolov, C. Reese and Z. Bao, *Nat. Mater.*, 2010, **9**, 859–864.
25 M. Ying, A. P. Bonifas, N. Lu, Y. Su, R. Li, H. Cheng, A. Ameen, Y. Huang and J. A. Rogers, *Nanotechnology*, 2012, **23**, 344004.
26 H.-K. Lee, S.-I. Chang and E. Yoon, *J. Microelectromech. Syst.*, 2006, **15**, 1681–1686.
27 A. Petropoulos, G. Kaltsas, D. Goustouridis and E. Gogolides, *Procedia Chem.*, 2009, **1**, 867–870.
28 X. Liu, Y. Zhu, M. W. Nomani, X. Wen, T.-Y. Hsia and G. Koley, *J. Micromech. Microeng.*, 2013, **23**, 025022.
29 C. Metzger, E. Fleisch, J. Meyer, M. Dansachmüller, I. Graz, M. Kaltenbrunner, C. Keplinger, R. Schwödiauer and S. Bauer, *Appl. Phys. Lett.*, 2008, **92**, 013506.

30 G. Barrett and R. Omote, *Inf. Disp.*, 2010, **26**, 16–21.
31 T. G. Zimmerman, J. R. Smith, J. A. Paradiso, D. Allport, and N. Gershenfeld, *Proceedings of the SIGCHI Conference on Human Factors in Computing Systems*, ACM Press/Addison-Wesley Publishing Co., 1995, pp. 280–287.
32 S. Takamatsu, T. Takahata, M. Muraki, E. Iwase, K. Matsumoto and I. Shimoyama, *J. Micromech. Microeng.*, 2010, **20**, 075017.
33 D. Choi, K. Y. Lee, K. H. Lee, E. S. Kim, T. S. Kim, S. Y. Lee, S.-W. Kim, J.-Y. Choi and J. M. Kim, *Nanotechnology*, 2010, **21**, 405503.
34 I. Jung, J. Xiao, V. Malyarchuk, C. Lu, M. Li, Z. Liu, J. Yoon, Y. Huang and J. A. Rogers, *Proc. Natl. Acad. Sci. U. S. A.*, 2011, **108**, 1789.
35 X. Huang, W.-H. Yeo, Y. Liu and J. A. Rogers, *Biointerphases*, 2012, **7**, 52.
36 X. Zhao and Z. Suo, *Phys. Rev. Lett.*, 2010, **104**, 178302.
37 H. Stoyanov, P. Brochu, X. Niu, E. D. Gaspera and Q. Pei, *Appl. Phys. Lett.*, 2012, **100**, 262902.
38 M. Kubo, X. Li, C. Kim, M. Hashimoto, B. J. Wiley, D. Ham and G. M. Whitesides, *Adv. Mater.*, 2010, **22**, 2749–2752.
39 J.-H. So, J. Thelen, A. Qusba, G. J. Hayes, G. Lazzi and M. D. Dickey, *Adv. Funct. Mater.*, 2009, **19**, 3632–3637.
40 C. Yu, C. Masarapu, J. Rong, B. Wei and H. Jiang, *Adv. Mater.*, 2009, **21**, 4793–4797.
41 Z. Fan, H. Razavi, J. Do, A. Moriwaki, O. Ergen, Y.-L. Chueh, P. W. Leu, J. C. Ho, T. Takahashi, L. A. Reichertz, S. Neale, K. Yu, M. Wu, J. W. Ager and A. Javey, *Nat. Mater.*, 2009, **8**, 648–653.